Bio-preparation of CuO@ZnO Nanocomposite *via* Spent Mushroom Substrate and its Application against *Candida albicans* with Molecular Docking Study

Emad Abada,[a,*] Tarek M. Galal,[b] Amani Alhejely,[c] Abeer Mahmoud Mohammad,[c] Yasir Alruwaili,[d,e] Mohammed S. Almuhayawi,[f,g] Abdel-Rahman M. Shater,[a] Mohammed H. Alruhaili [f,h], and Samy Selim,[d,*]

Green routes for the bio-designing of bicomponent nanocomposites and their utilizations have attracted many investigators. Bio-designing of CuO@ZnO nanocomposites was performed using spent mushroom substrate (SMS). Ultraviolet-spectrophotometry, transmission electron microscopy, Fourier transform infrared (FT-IR), and energy dispersive X-ray (EDX), besides X-ray diffraction (XRD) were exploited to characterize the synthesized CuO@ZnO. The dimensions of CuO@ZnO nanocomposites ranged from 31.4 and 95.9 nm. Both FT-IR and EDX analyses displayed the presence of some organic constituents from the SMS that joined to the surface of the fabricated CuO@ZnO nanocomposite. CuO@ZnO nanocomposite succeeded in inhibiting *Candida albicans* with an inhibition zone of 33.5 ± 2 mm. *C. albicans* biofilm was affected by CuO@ZnO nanocomposite with biofilm inhibition of 25.08, 68.70, and 88.56% at 25, 50, and 75% of minimum inhibitory concentration, respectively. Molecular docking studies showed substantial binding affinities, as well as common hydrogen bonds. Optimum binding sites for CuO and ZnO nanoparticles were found to have binding affinities of interactions with 4YDE, 3DRA, and 1EAG proteins of *C. albicans*, resulting in, respectively, -2.7942, -3.30097, and -2.52129 kcal/mol, and -3.78244, -4.6029, and -4.1352 kcal/mol values. The findings suggest that CuO@ZnO nanocomposite can effectively suppress *C. albicans* growth.

DOI: 10.15376/biores.19.3.6670-6689

Keywords: Nanocomposite; Green synthesis; Compost; Candida albicans; Docking interactions

*Contact information: a: Department of Biology, College of Science, Jazan University, P.O. Box. 114, Jazan 45142, Kingdom of Saudi Arabia; b: Department of Biology, College of Sciences, Taif University, P.O. Box 11099, Taif 21944, Saudi Arabia; c: Department of Biology, College of Aldarb, Jazan University, P.O. Box. 114, Jazan 45142, Kingdom of Saudi Arabia; d: Department of Clinical Laboratory Sciences, College of Applied Medical Sciences, Jouf University, Sakaka 72388, Saudi Arabia; e: Sustainable Development Research and Innovation Center, Deanship of Graduate Studies and Scientific Research, Jouf University, Sakaka 72388, Saudi Arabia; f: Department of Clinical Microbiology and Immunology, Faculty of Medicine, King Abdulaziz University, Jeddah 21589, Saudi Arabia; g: Yousef Abdulatif Jameel Scientific Chair of Prophetic Medicine Application, Faculty of Medicine, King Abdulaziz University, Jeddah 21589, Saudi Arabia; h:Special Infectious Agents Unit, King Fahad Medical Research Center, King AbdulAziz University, Jeddah, Saudi Arabia; *Corresponding author: eabada@jazanu.edu.sa* (AA), *sabdulsalam@ju.edu.sa* (SS)*

INTRODUCTION

In the last decade, nanotechnology has represented an effective technology across various fields (Alsolami *et al.* 2023; Alghonaim *et al.* 2024a). Nanotechnology is continually being developed to suit modern applications and is being used to solve many medical, environmental, agricultural, and food problems (Al-Rajhi and Abdelghany

2023a,b). The scientific community is paying increased attention to metal oxide nanoparticles (NPs) to address several problems such as microbial resistance to drugs, contamination with dyes, and water purification (Al Abboud *et al.* 2024). These NPs have special qualities like high surface-to-volume ratio, little toxicity, and stability. These characteristics enable these NPs to perform their functions with high efficiency. Also, they can be produced *via* a variety of different physical and chemical routes (Salama *et al.* 2021).

Green synthesis methods that make use of eco-friendly substrates or microorganisms have been acknowledged as a potentially effective strategy to overcome the drawbacks associated with the aforementioned approaches (Abdelghany *et al.* 2018). Because of their availability, affordability, and biocompatibility, microorganisms have been the topic of essential investigation and development in the previous few years for the fabrication of metallic nanoparticles and various metal oxides. Inorganic functional NPs, such as SeO, TiO_2, ZnO, and CuO, have been reported in multiple reports (Al-Rajhi *et al.* 2022a; Abdelhady *et al.* 2024a; Alghonaim *et al.* 2024b,c). Zinc and copper oxides, which are among those mentioned NPs, are two widely used metal oxide types of semiconductors. These NPs can prevent the development of filamentous and unicellular molds, as well as Gram-positive and Gram-negative bacteria (Alsalamah *et al.* 2023a; Abdelhady *et al.* 2024b). The primary benefit of inorganic antimicrobial agents over organic ones is their high stability and robustness at elevated temperatures. Numerous factors, including surface area, particle size, crystallinity, dose, pH, shape, and the type of tested microorganisms, are indicative of these metallic nanoparticles' antimicrobial activity (Abdelghany *et al.* 2020). The FDA (Food and Drug Administration, USA) has recently classified both ZnO and CuONPs as safe inorganic compounds. Because of its favorable exciton binding energy, abundance, low cost, and nontoxicity, ZnO is one of the oxides that have been investigated the utmost for wastewater management (Ullah *et al.* 2021).

Several medicinal utilizations have been associated with ZnO-NPs; however, further developed approaches are required for enhancing these applications such as antimicrobial activities (Abdelghany *et al.* 2023a). To achieve this improvement, the functionality and characteristics of ZnO-NPs can be developed by joining them to other dopant constituents, such as biomolecules or transition metals, at nanoscale form (Khan *et al.* 2017; Qanash *et al.* 2023). After joining or doping with the dopant constituents, the NPs surfaces are modified to possess good biocompatibility to efficiently achieve biological activities, for instance, antimicrobials, drug delivery systems, antioxidants, biosensors, and bio-imaging (Kalantar *et al.* 2013). The properties of either physical or biological ZnO-NPs were found to be significantly modified by Cu^{2+} as the dopant transition metal. Cu^{2+} was reported as the best selection for enhancing the biomedical application of ZnO-NPs (Wahab *et al.* 2013). The inhibitory potential of combined CuO and ZnO was studied against microorganisms *via* fixing Cu into a ZnO matrix or the reverse (Khalid *et al.* 2021).

Many researchers have previously utilised ZnO tagged with CuO for antibacterial applications (Al-Rajhi *et al.* 2022b; Mandal *et al.* 2024). According to Sandhya and Kalaiselvam (2021), CuO/ZnO nanocomposite demonstrated antimicrobial properties *versus Streptococcus aureus*, *Bacillus subtilis*, *Escherichia coli*, *Shigella* sp., *Aspergillus niger*, and *Candida albicans*. CuO/ZnO nanocomposite was synthesized *via* natural materials of plants and showed more antibacterial potential than ZnONPs *versus E. coli* and *S. aureus* (Mohammadi-Aloucheh *et al.* 2018). In another study, *Klebsiella pneumonia*, *Streptococcus pyogenes*, and *S. aureus*, besides *E.coli* were inhibited by Cu-doped ZnO-NPs with clear zones varying from 11 to 24 mm (Khalid *et al.* 2021).

Molecular docking is becoming a key method in drug discovery. It is the standard tool for identifying active binding sites between proteins and ligands. The major use of construction-based virtual checking is to detect unique constituents active for specific protein targets, which has resulted in significant advancements (Yahya *et al.* 2022; Alsalamah *et al.* 2023a).

The genus *Candida* comprises roughly 200 species. A few numbers of species are commensals, meaning they only infect humans when their immune systems have been weakened. In contrast, these infections can be superficial, leading to mucocutaneous candidiasis diseases, or they can spread to internal organs and blood circulation, resulting in invasive, potentially fatal candidiasis diseases (Hemaid *et al.* 2021; Alsalamah *et al.* 2023b).

In the mushroom cultivation process, once the sporocarp is detached from the culture, spent mushroom substrate (SMS), a composted organic medium that is the end metabolite of the mushroom-cultivation development, is the primary by-product in the mushroom production. The agro-remains and hyphae of fungi left over after collecting the mushrooms are referred to interchangeably as SMS. Among other renewable agricultural residues, this waste is typically composed of sawdust, sugarcane bagasse, horse manure with wheat straw bedding, hay, ground corncobs, poultry manure, gypsum, cottonseed meal, and cocoa shells (Antunes *et al.* 2020; Alghonaim *et al.* 2023; Al-Rajhi *et al.* 2023c). The SMS was previously applied in several environmental and biological applications. Therefore, in the current work, SMS was applied as an intermediary for preparing CuO@ZnO nanocomposite with studying its biological activity against *C. albicans in vitro* and *in silico.*

EXPERIMENTAL

Utilized Source in the Bio-designing of CuO@ZnO Nanocomposite

The SMS was collected after harvesting the mushroom fruits (*Pleurotus sajor-caju*). Rice straw was utilized as compost for mushroom cultivation. The collected SMS was desiccated for 48 h at 60 ℃. The dried SMS was ground to obtain fine powder. A total of 25 g of the obtained powder was then combined with 200 mL of deionized H_2O in a water bath (for to 2 h at 80 ℃). The obtained mixture was filtered *via* a size pore of 11 µm a filter paper. The filtrate was as extract and applied for bio-preparation of CuO@ZnO nanocomposite.

Preparation of the CuO@ZnO Nanocomposite

A total of 25 mL of SMS extract was mixed with 100 mL of $Zn(CH_3CO2)_2.2H_2O$ (18.35 g, 0.1 mol) and was employed to prepare CuO@ZnO nanocomposite with a mole ratio of 1:5. Next, NaOH solution was added dropwise to the mixture to bring its pH to 10. A white solution was visible after 30 min of vigorous mixing and heating of the resultant mixture. After that, at 85 °C, the stirring mixture was gradually mixed with a 50 mL solution of $CuSO_4$ $5H_2O$ (3.19 g, 0.02 mol), which turned a dark green color. The blend was stirred for 2 h. After washing, centrifuging for 15 min at 10,000 rpm, drying in an oven at 50 °C, and 2 h of calcination at 400 °C in a furnace, this mixture was collected.

Characterization CuO@ZnO Nanocomposite

The CuO@ZnO nanocomposite was characterized *via* several instruments namely X-ray diffraction (XRD) (Shimadzu 7000 Diffractometer), transmission electron microscopy (TEM) (Philips CM-200, Japan), and UV–Vis spectroscopy, besides Energy dispersive x-ray (EDX) combined with scanning electron microscopy (SEM-JEOL JSM 840A, China), and Fourier transform-infrared (FT-IR).

Efficacy of CuO@ZnO Nanocomposite against *C. albicans* Growth

The radius of inhibition zones was quantified using the agar well diffusion experiment to assess the CuO@ZnO nanocomposite extract's antiyeast effects. *Candida albicans* (ATCC 10221), suspension at a concentration of 10^6 cfu/mL was inoculated onto an Oxoid Sabouraud Dextrose plate containing agar, followed by incubation at 30 ºC for a full day. The DMSO solution was used to dilute 20 µL of CuO@ZnO nanocomposite onto 5 mm of agar well. Nystatin (30 µg/mL) was employed as the control (positive), whereas the DMSO (Dissolver) was employed as the control (negative). Next, the culture media was injected with yeasts and incubated for 24 to 30 h at 37 °C. Using a caliper, the area of the growth inhibition zones surrounding each paper disc was documented (Abdel-Ghany 2013).

Minimum Inhibitory Concentration (MIC) Assessment of CuO@ZnO Nanocomposite

Tests were conducted on CuO@ZnO nanocomposite to determine their minimum inhibitory concentration against *C. albicans*. Based on the CLSI M27-A3 standard protocol, *C. albicans* was diluted to a concentration equal to 0.5 McFarland. Employing 96-well plates, 100 µL of medium broth (pH 7, modified by a buffer of MOPS) were relocated into wells. In the first column's wells, 100 µL of CuO@ZnO nanocomposite (1 mg/mL) was combined with medium broth before serial dilution was carried out. Each well received 100 µL (0.5 McFarland) of the *C. albicans* cell suspension; wells without the cell suspension served as the negative control. Afterwards, there was a one-day incubation period at 35 ℃. The lowest dose of CuO@ZnO nanocomposite that causes 50% inhibition of *C. albicans* growth was termed as MIC.

Minimum Fetal Concentration (MFC) Assessment of CuO@ZnO Nanocomposite

Using Sabouraud Dextrose Agar plates, 50 µL suspension of the clear homogenised well (without any visible *C. albicans* development) was cultured to measure the MFC. This was then incubated for 48 h at 35 ℃. Once compared to growth at control, the lowest quantity of CuO@ZnO nanocomposite caused 99.9% of growth inhibition. This was observed in MFC growth. Each yeast colony's count (measured in CFU/mL) at various amounts was paralleled to the total counts of the *C. albicans* colonies at treatment-free.

Efficacy of CuO@ZnO Nanocomposite Against *C. albicans* Biofilm Formation

Efficacy of CuO@ZnO nanocomposite against *C. albicans* biofilm development was valued in 96-well polystyrene flat bottom plates. The tested *C. albicans* was adjusted at 10^5 CFU/mL and inoculated in the wells of microplate amended with the different sub-lethal dosages (MFC of CuO@ZnO nanocomposite) ranged from 25 to 75%. At 30 °C, the inoculated plates were kept for 2 days, and subsequently the supernatant was separated to

allow the free-floating cells to be washed by sterile distilled H_2O in each well. The formed *C. albicans* was stained for 15 min by 0.1% aqueous crystal violet. The stained plate was left for 30 min to air dry. Water was then employed to eliminate any additives of crystal violet. The joined dye to the *C. albicans* cells was dissolved by 200 µL of 95% ethanol to each well for 10 min. Subsequently, microplate reader was operated to register the absorbance at 570 nm. Wells without CuO@ZnO nanocomposite were served as control. Anti-biofilm activity was estimated using the equation below:

$$\text{Anti} - \text{biofilm activity } (\%) = \left(\frac{\text{Control absorbance} - \text{CuO@ZnO nanocomposite absorbance}}{\text{Control absorbance}}\right) \times 100$$

Molecular Docking Interaction of CuO and ZnO Nanoparticles with *C. albicans* Proteins

Docking processes were simulated utilizing the Molecular Orbital Environment (MOE) program to examine the action of CuO and ZnO NPs *versus* the crystal construction of *C. albicans* proteins. To find out the inhibitory potential of tested molecules, 3D structures of major target receptors were acquired from the Protein Data Bank (PDB) (www.rcsb.org) with codes namely 4YDE, 3DRA, and 1EAG. Atoms of hydrogen were added once the molecules of water around the protein had been detached. The parameters and charge values were calculated employing the force field of MMFF94x. After generating α-site spheres with MOE's site finder module, the CuO-NPs' and ZnO-NPs' structures were modeled using the Gaussian 09 program (Frisch 2009) and exported as MOL files (.mol) for MOE appearance. The compounds were docked at the active site employing MOE's DOCK module. The dock score for the program of MOE was decided employing the London dG scoring technique, with location as a triangle matcher, retention as ten, and refining as a force field. Docked ligands' leading conformations were detected *via* examining the values of RMSD, binding modes, and binding energies, in addition to the specified remains.

RESULTS AND DISCUSSION

The SMS succeeded as a natural mediator for the creation of CuO@ZnO nanocomposite. This may be due to the presence of several enzymes, in addition to primary and secondary metabolites in the SMS, as mentioned previously. According to several studies, both wild and cultivated mushrooms have been employed for the creation of numerous NPs. Though the creation of NPs in the presence of mushroom substrate appears to take place simply, numerous factors determine its stability as well as biocompatibility such as temperature, reaction medium pH, composition of medium, and quantity of biomass (Rafeeq *et al.* 2021; Gur *et al.* 2022). The NPs synthesis mechanisms according to previous studies may be due to different kinds of enzymes, such as reductases in the metabolized substrate, that can be employed for the NPs reduction and stabilization (Papoutsis *et al.* 2020). Moreover, exudates of mushrooms have been found to contain several biomolecules such as alkaloids, amino acids, acids, flavonoids, phenols, saccharides, steroids, saponins, and vitamins, besides other metabolites (Antunes *et al.* 2020; Elsakhawy *et al.* 2022). The absorption of CuO@ZnO nanocomposite and extract in the UV−vis spectra are illustrated (Fig. 1A). CuO@ZnO nanocomposite absorbed intensely (λ_{max} = 378 nm), which is harmonious with other scientific papers that recorded an

absorption peak at 374 nm (Zhu *et al.* 2018; Bekru *et al.* 2022). From TEM imaging, CuO@ZnO nanocomposite appeared as spherical NPs with different sizes of 31.4 and 95.9 nm (Fig. 1 B) with average size 57.22± 17.65 mm (Fig. 1 C) indicating the existence of bicomponent NPs of CuO@ZnO nanocomposite. According to Khalid *et al.* (2021), the Cu additive may alter and control the size and shape of ZnO NPs. Yousefinia *et al.* (2023) recorded a maximum absorbance wavelength at 392 nm for green synthesized ZnO/CuO nanocomposite *via* an extract of *Berberis vulgaris*.

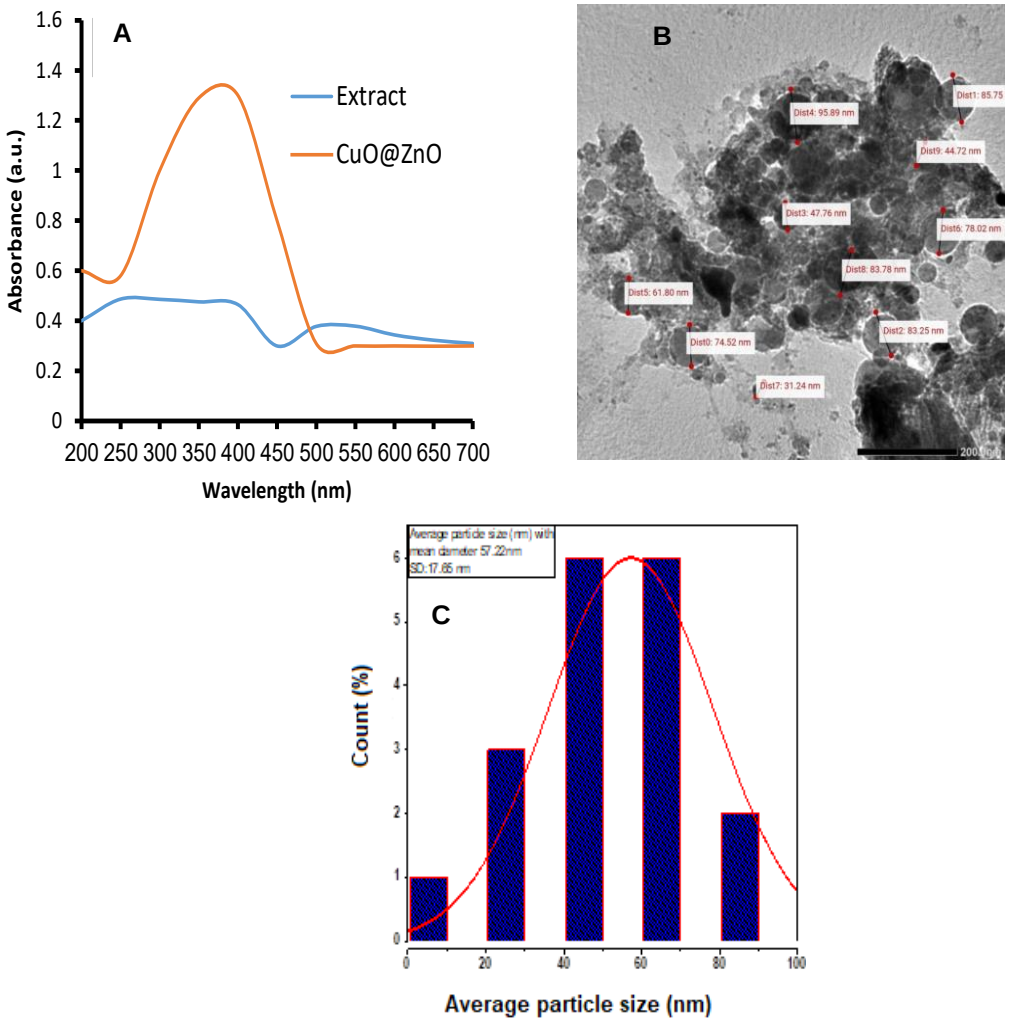

Fig. 1. (A) UV–Vis spectroscopy of SMS extract and CuO@ZnO nanocomposite, (B) CuO@ZnO nanocomposite characterization by TEM, (C) Average particle size

The use of FT-IR confirmed that functional groups were present on the biosynthetic CuO@ZnO nanocomposite surface (Fig. 2).

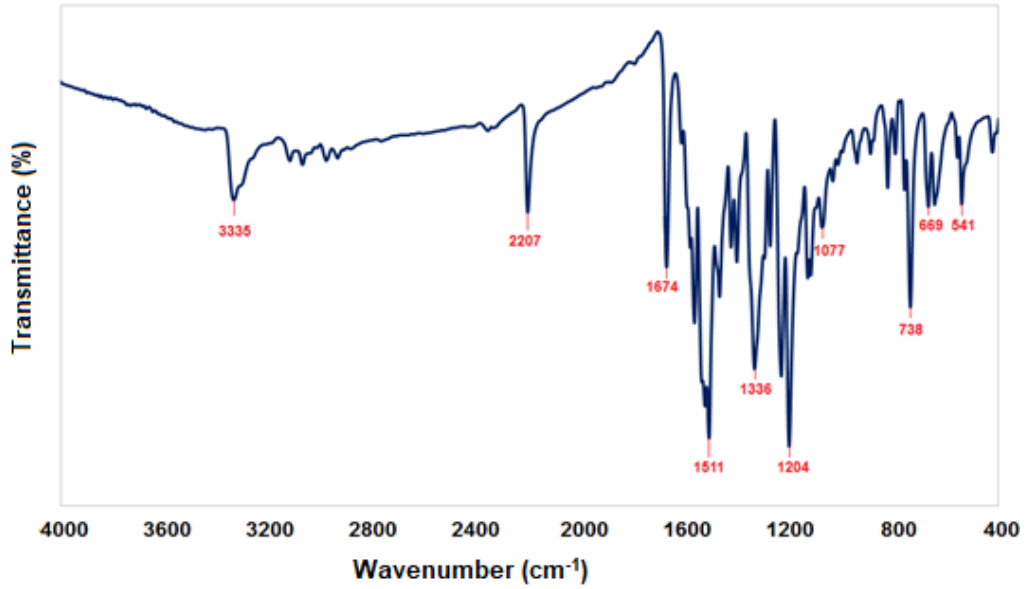

Fig. 2. Spectra of CuO@ZnO nanocomposite *via* FT-IR

The representative peak of the amide I band (C = O stretch/hydrogen bond attached with COO–) appeared at a frequency of 1674 cm^{-1} (Fig. 2). In contrast, the amide II band (NH bending attached to CN stretching) is assigned to frequencies of 1511, 1336, and 1204 cm^{-1} (COO– symmetrical stretching). They can be attributed to the bands at 1336 and 1204 cm^{-1} to CH_2. The C-O stretching occurrence at 1077 cm^{-1} is linked to a band of the amide III. They are associated with the peaks at 3335 and 2207 cm^{-1} to OH and -COO stretching, respectively. The metal–oxygen vibration (Cu–O as well as Zn-O) is represented by the peak positions at 541, 669, and 738 cm^{-1} frequencies (Abdelghany *et al.* 2023; El-Khawaga *et al.* 2023).

The crystalline construction of CuO@ZnO nanocomposite was analyzed by XRD spectrometry (Fig. 3). The sample contained two distinct components, CuO (with JCPDS 05-0661) and ZnO (with JCPDS 36-1451), without any additional impurity peaks (BaQais *et al.* 2023). CuO@ZnO nanocomposite showed peaks emerged at 2θ = 47.76, 63.11, 68.18, 72.71, and 77.48° matching to planes (202, 113, 220, 311, and 222, correspondingly) of the crystal construction of CuO (Shaheen *et al.* 2021). Contrastingly, the plane of ZnO crystal structure peaks emerged at 2θ = 31.9, 34.59, 36.39, 56.79, 66.59, and 69.1°, which corresponded to (100), (002), (101), (110), (200), and (201) (El-Khawaga *et al.* 2023). CuO@ZnO nanocomposite diffractogram does not tell the presence of further impurities. It certifies that the CuO@ZnO nanocomposite was fabricated in pure form.

As visualized in Fig. 4, SEM imaging was used to assess the surface shape of CuO@ZnO nanocomposite. The CuO@ZnO nanocomposite was almost perfectly spherical in shape. The elemental makeup of the CuO@ZnO nanocomposite powder was ascertained by EDX analysis. The CuO@ZnO nanocomposite's EDX spectra showed the presence of multiple distinct elements linked to the component's carbon [C], oxygen [O], zinc [Zn], and copper [Cu] (Fig. 4). The metabolite sample's carbon [C], in contrast to the copper [Cu], zinc [Zn], and oxygen [O] indicators, point to the formation of a CuO-ZnO nanocomposite.

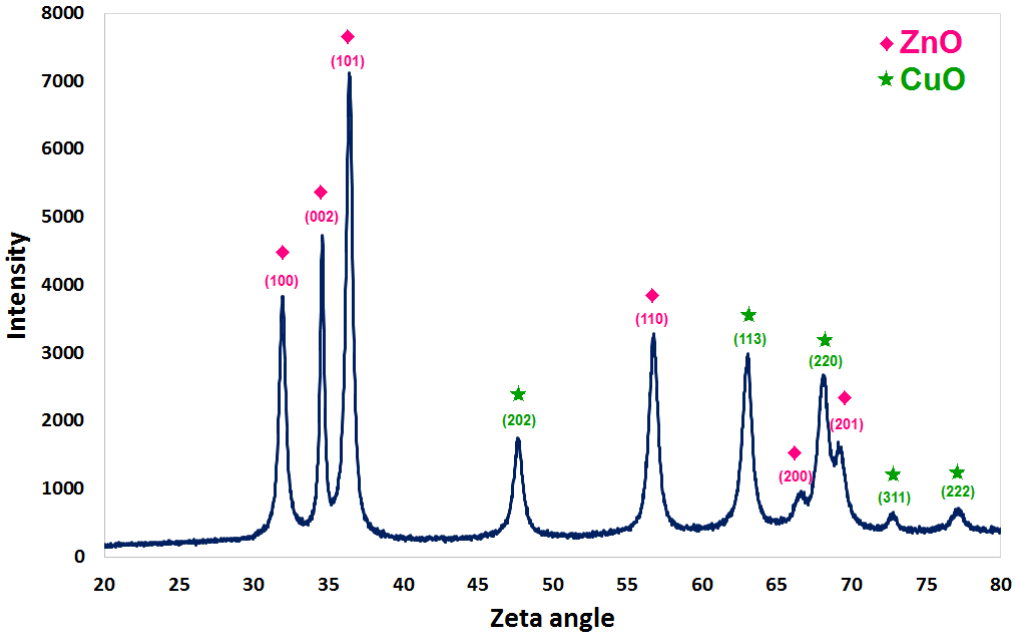

Fig. 3. XRD chromatogram of fabricated CuO@ZnO nanocomposite

Anti-yeast Activity

CuO@ZnO nanocomposite exhibited inhibitory action against *C. albicans* with more inhibition zone of 33.5 ± 2 mm than the positive control (Nystatin), which reflected an inhibition zone of 31.3 ± 2 mm (Table 1 and Fig. 5 A). In a recent report, a composite of CuONPs with nanochitosan and nanostarch exhibited anti-yeast activity against *C. tropicalis* and *C. glabrata* with 28- and 27-mm inhibition zones, respectively (Saied *et al.* 2023). In a previous investigation, nystatin recorded an inhibition zone that ranged from 18 to 24 mm against *C. albicans* (Khoshkholgh-Pahlaviani *et al.* 2013). Besides antifungal activity, CuO@ZnO nanocomposite exhibited bactericidal activities towards *S. aureus* and *E. coli*. Moreover, its antimicrobial potential was affected by the dose of CuO in the nanocomposite and improved by increasing its dose (Mohammadi-Aloucheh *et al.* 2018). The antimicrobial potential mechanism of CuO@ZnO nanocomposite was described (Lam *et al.* 2018), which is represented by the rupture of the membrane of cell and disorganization of cell wall. The MIC and MFC of CuO@ZnO nanocomposite were recorded against *C. albicans* with values of 31.25 and 125 µg/mL, respectively (Table 1). From a recent study (Yousefinia *et al.* 2023), CuO@ZnO nanocomposite revealed excellent activity toward *C. albicans*, where MIC and MFC were 31.2 and 125 µg/mL. Additionally, filamentous fungi including *Neoscytalidium dimidiatum*, *Magnaporthe oryzae*, *Penicillium*, and *Aspergillus* were inhibited by CuO@ZnO nanocomposite with the low MIC of 10 mg/mL (Uyen *et al.* 2020). The formation of *C. albicans* biofilm successively declined with increasing CuO@ZnO nanocomposite concentration (Table 1 and Fig. 5B). At 25%, 50%, and 75%, the anti-biofilm activity was 25.08, 68.70, and 88.56%, respectively. The results of biofilm formation can perhaps explain the anti-adhesion and then the anti-biofilm potentials of CuO@ZnO nanocomposite.

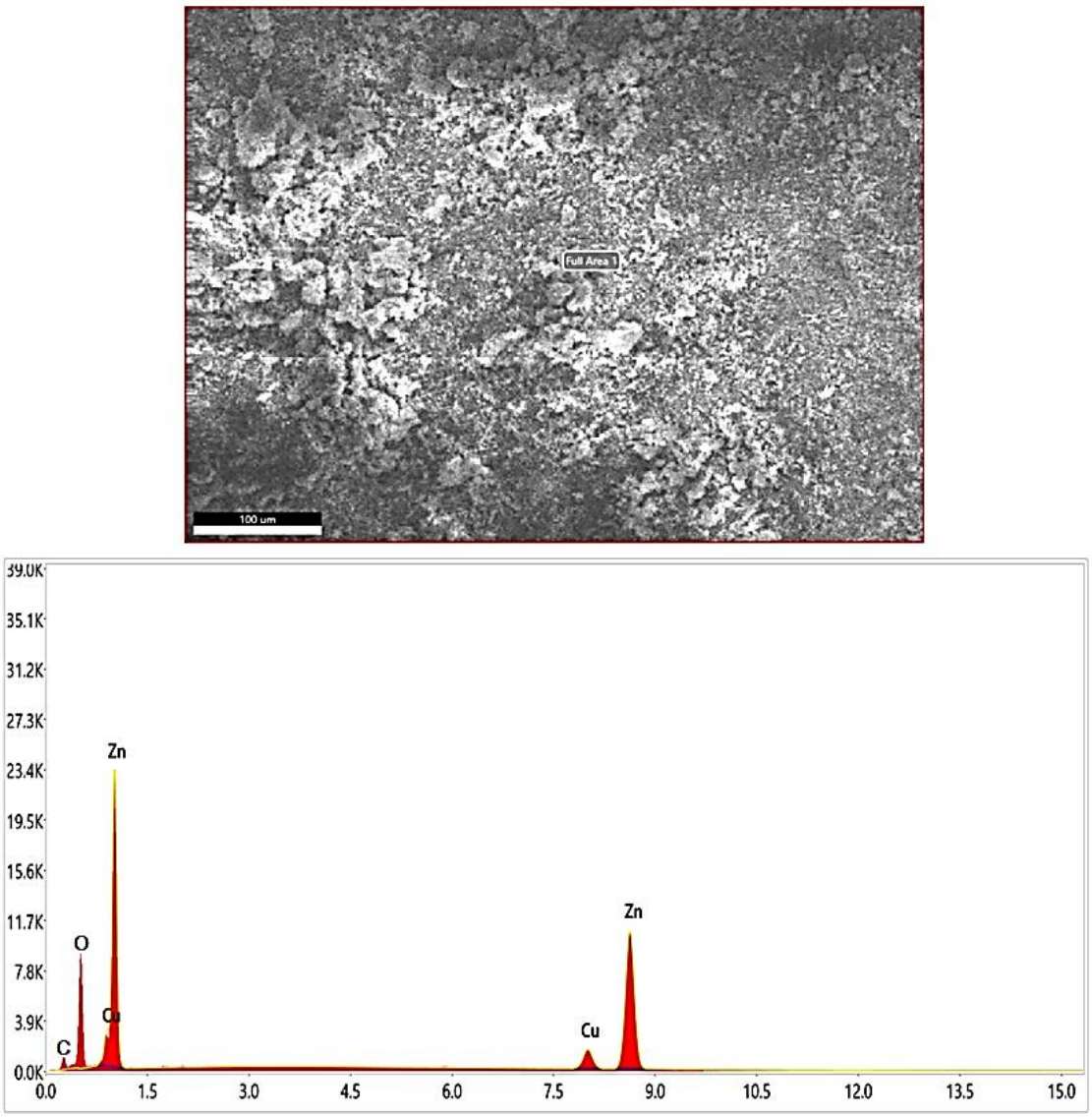

Fig. 4. SEM-EDX analysis of CuO@ZnO nanocomposite

Table 1. Inhibitor, MIC, MFC, and Anti-biofilm Potential of CuO@ZnO Nanocomposite against *C. albicans*

Inhibition Zone (mm)		CuO@ZnO Nanocomposite		Anti-biofilm of CuO@ZnO Nanocomposite at			
CuO@ZnO Nanocomposite	Positive Control	MIC (µg/mL)	MFC (µg/ML)	0%	25%	50%	75%
33.5 ± 2	31.3 ± 1	31.25	125	0.0	25.08	68.70	88.56

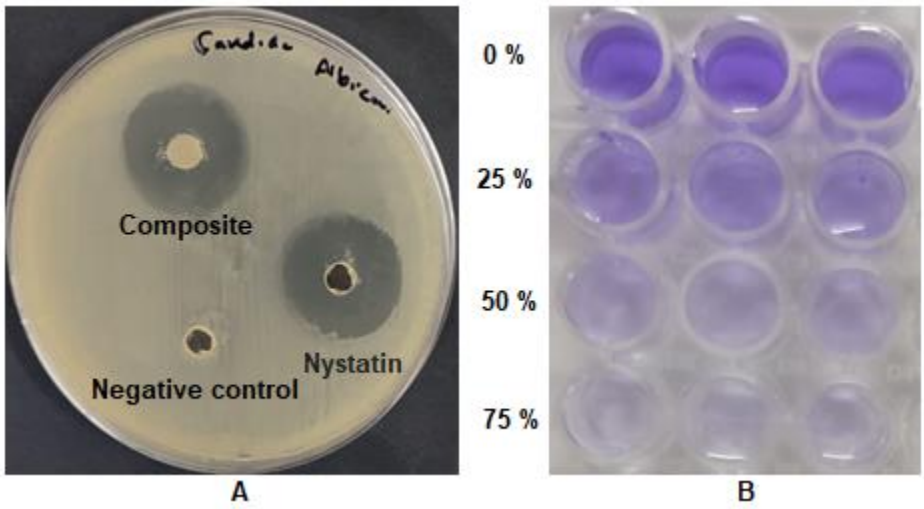

Fig. 5. (A) Inhibition zone of *C. albicans* exposed to CuO@ZnO nanocomposite (composite), Nystatin, and DMSO (negative control); (B) Microtiter plate presented color alteration as a marker of declined *C. albicans* biofilm. Media + *C. albicans* (0%), Media + *C. albicans* + 25% of MBC of ZnO@CuO nanocomposite, Media + *C. albicans* + 50% of MBC of CuO@ZnO nanocomposite and Media + *C. albicans* + 75% of MBC of CuO@ZnO nanocomposite

Molecular docking is a valuable technique in drug design, as it can explain how proteins interact with ligands to produce stable complexes with significant biological effects. Three *Candida albicans* proteins were chosen based on their ability to bind successfully to the proposed medication. CuO-NPs and ZnO-NPs effectively inhibit enzymes and, in additional instances, activate them, leading to the demise of three proteins tested (4YDE, 3DRA, and 1EAG). ZnO-NPs demonstrated better binding affinities (best posture) of -3.78244, -4.6029, and -4.1352 kcal/mol for interacting with 4YDE, 3DRA, and 1EAG than CuO-NPs, suggesting their ability to inhibit the target receptors. 3DRA also has a higher average binding affinity than the other target proteins. The outcomes include conformer energy (E_conf), binding energy scores (S), and root-mean-square deviation (rmsd). The placement stage score (E_place), the rescoring stages 1 and 2 scores (E_scores 1 and 2), and the refinement stage score (E_refine) that were calculated according to the Generalised Born solvation model's (GB/VI) refinement score were determined by adding the solvation energies and van der Waals electrostatics (Table 2). ZnO-NPs interact toward the protein receptors pocket 3DRA through GLU 262 amino acid residue *via* Zn 2, Zn 4, O 1, O 3, and O 5. Several interactions of tested compounds with amino acids were inside the target pocket of proteins (Table 3). They maintained their position in the protein central binding position by modulating several electrostatic connections, as demonstrated in the biological activity profile (Figs. 6 through 11) with the illustrative basic for the kinds of contact among nanocomposite and receptors of protein (Fig. 12). Molecular docking of Cu-doped ZnO nanocomposite was studied with Penicillin-binding proteins of *S. aureus* (Binding score of − 7.90 kcal/mol) (El-Sayed *et al.* 2024). In another report, binding score (− 4.981 kcal/mol) resulted from the docking study among Ag–Cu nanocomposite and *β*-lactamase enzyme of bacteria (Mureed *et al.* 2021).

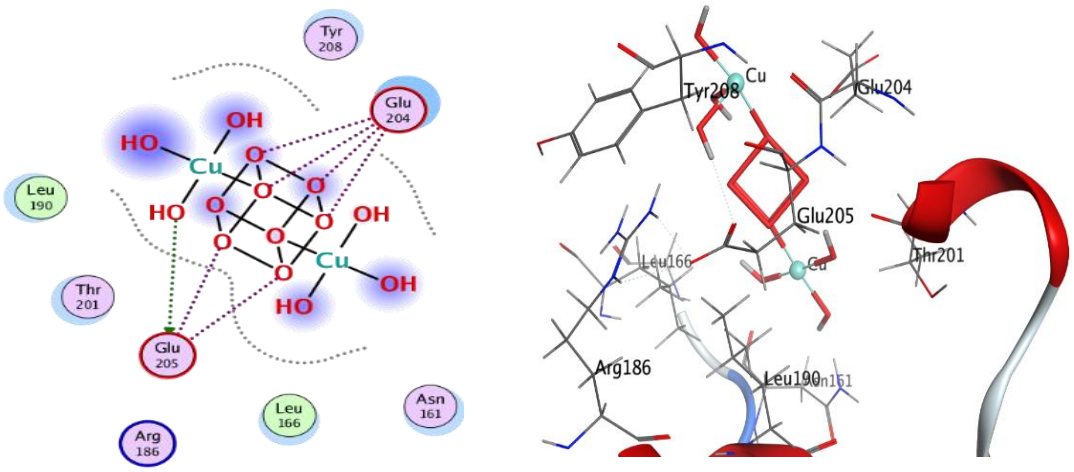

Fig. 6. Diagrams (2D and 3D) display the interaction among CuO-NPs and active positions of 4YDE protein

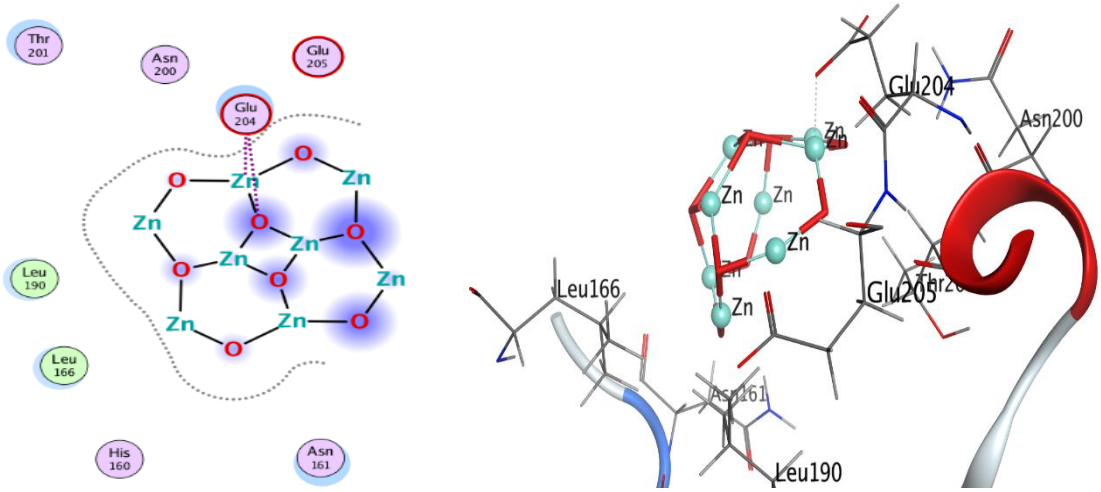

Fig. 7. Diagrams (2D and 3D) display the interaction among ZnO-NPs and active positions of 4YDE protein

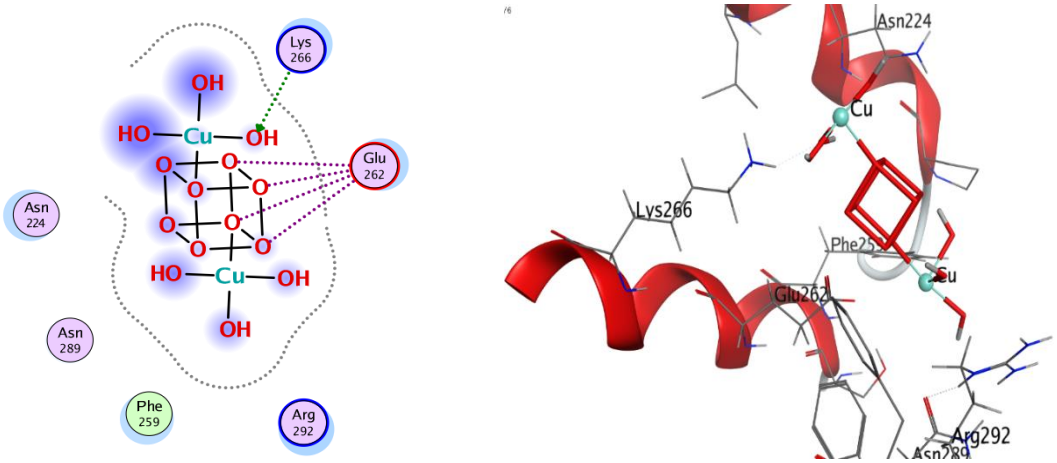

Fig. 8. Diagrams (2D and 3D) display the interaction among CuO-NPs and active positions of 3DRA protein

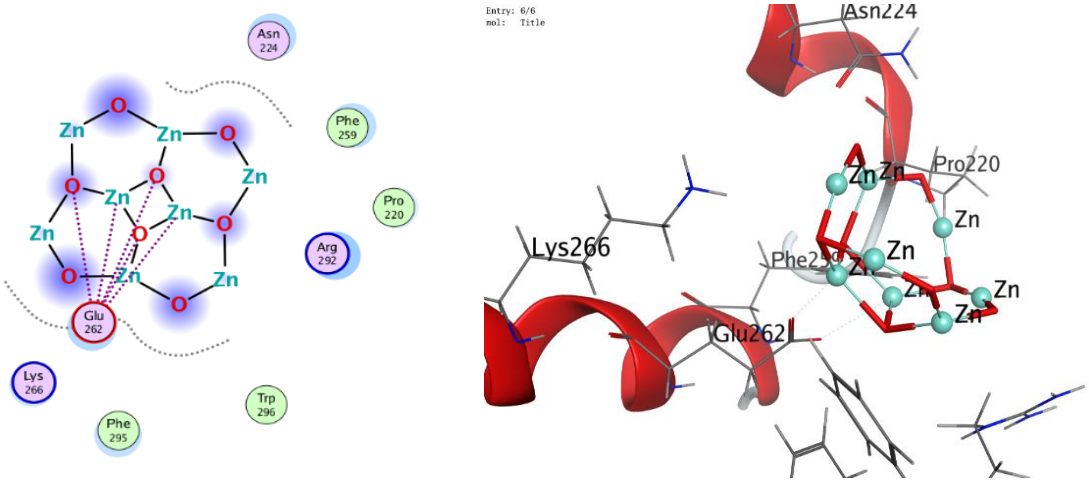

Fig. 9. Diagrams (2D and 3D) display the interaction among ZnO-NPs and active positions of 3DRA protein

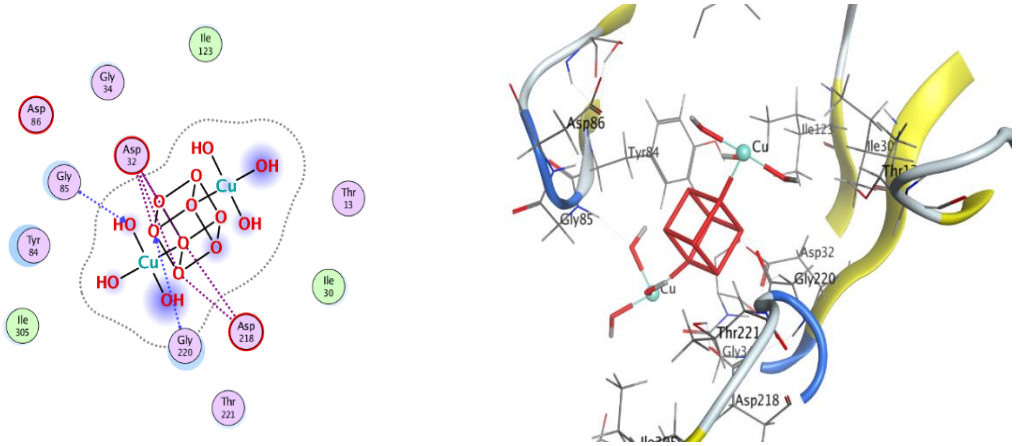

Fig. 10. Diagrams (2D and 3D) display the interaction among CuO-NPs and active positions of 1EAG protein

Table 2. Docking Scores and Energies of CuO-NPs and ZnO-NPs with *C. albicans* (PDB ID:4YDE, 3DRA and 1EAG) Receptors

Mol	Protein	S	rmsd_refine	E_conf	E_place	E_score1	E_refine	E_score2
CuO-NPs	4YDE	-2.7942	1.22508	-1407.5	-73.0507	-6.43933	-7.98265	-2.7942
ZnO-NPs	4YDE	-3.78244	3.606388	-1116.44	-19.0773	-2.11585	-24.254	-3.78244
CuO-NPs	3DRA	-3.30097	3.520521	-718.008	-40.0055	-15.1086	-17.7131	-3.30097
ZnO-NPs	3DRA	-4.6029	2.082043	-1114.88	-5.2237	-10.0715	-38.943	-4.6029
CuO-NPs	1EAG	-2.52129	2.831452	-1412.1	-57.3039	-22.853	12.92917	-2.52129
ZnO-NPs	1EAG	-4.1352	3.649283	-1115.41	-26.8842	-7.20762	-28.2455	-4.1352

Table 3. Interaction of MnO-NPs and ZnO-NPs with *C. albicans* (PDB ID:4YDE, 3DRA and 1EAG) Receptors

Mol	Protein	Ligand	Receptor	Distance	E (kcal/mol)
CuO-NPs	4YDE	O 12	OE1 GLU 205 (A)	3.55	-0.7
		O 1	OE1 GLU 204 (A)	2.76	-6.3
		O 3	OE1 GLU 205 (A)	3.27	-2.9
		O 4	OE1 GLU 204 (A)	2.81	-5.8
		O 5	OE1 GLU 204 (A)	2.87	-5.4
		O 7	OE1 GLU 205 (A)	3.26	-2.9
		O 8	OE1 GLU 204 (A)	2.98	-4.6
ZnO-NPs	4YDE	ZN 7	OE1 GLU 204 (A)	2.12	-3.1
		O 3	OE1 GLU 204 (A)	2.95	-4.8
CuO-NPs	3DRA	O 21	NZ LYS 266 (A)	2.85	-0.8
		O 1	OE1 GLU 262 (A)	2.78	-6.2
		O 1	OE2 GLU 262 (A)	3.39	-2.4
		O 4	OE1 GLU 262 (A)	2.98	-4.6
		O 4	OE2 GLU 262 (A)	2.77	-6.3
		O 5	OE1 GLU 262 (A)	2.57	-8.1
		O 8	OE1 GLU 262 (A)	2.86	-5.5
		O 8	OE2 GLU 262 (A)	3.73	-1.1
ZnO-NPs	3DRA	ZN 2	OE2 GLU 262 (A)	2.63	-0.7
		ZN 4	OE1 GLU 262 (A)	1.97	-5.4
		O 1	OE1 GLU 262 (A)	2.88	-5.3
		O 1	OE2 GLU 262 (A)	3.14	-3.6
		O 3	OE1 GLU 262 (A)	2.97	-4.7

		O 3	OE2 GLU 262 (A)	3.01	-4.4
		O 5	OE1 GLU 262 (A)	3.43	-2.2
CuO-NPs	1EAG	O 8	CA GLY 220 (A)	3.23	-1.0
		O 19	N GLY 85 (A)	2.92	-0.5
		O 5	OD1 ASP 32 (A)	3.47	-2.0
		O 5	OD2 ASP 32 (A)	2.70	-6.8
		O 6	OD1 ASP 32 (A)	3.49	-1.9
		O 6	OD2 ASP 32 (A)	3.50	-1.9
		O 6	OD2 ASP 218 (A)	3.64	-1.4
		O 7	OD1 ASP 32 (A)	3.03	-4.2
		O 7	OD1 ASP 218 (A)	3.56	-1.7
		O 7	OD2 ASP 218 (A)	2.75	-6.4
		O 8	OD1 ASP 32 (A)	2.86	-5.5
		O 8	OD2 ASP 32 (A)	3.23	-3.1
ZnO-NPs	1EAG	Zn 2	OD2 ASP 86 (A)	2.07	-2.8
		Zn 9	O GLY 220 (A)	2.67	-1.5
		O 1	OD1 ASP 86 (A)	3.21	-3.2
		O 1	OD2 ASP 86 (A)	3.66	-1.3
		O 3	OD1 ASP 86 (A)	3.34	-2.6
		O 3	OD2 ASP 86 (A)	3.04	-4.2
		O 6	OD2 ASP 86 (A)	3.14	-3.6

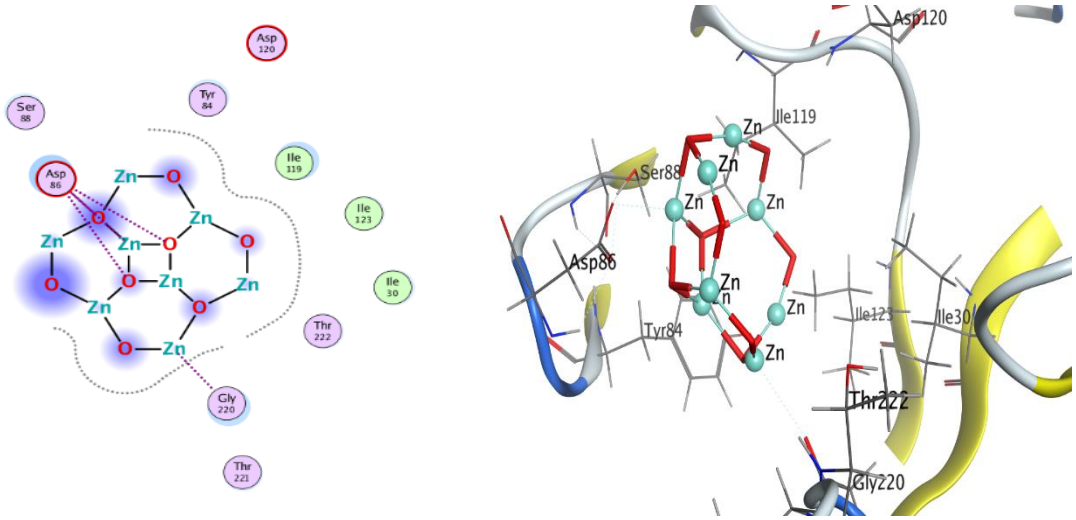

Fig. 11. Diagrams (2D and 3D) display the interaction among ZnO-NPs and active positions of 1EAG protein

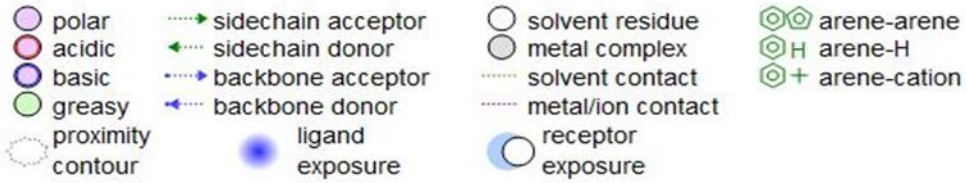

Fig. 12. The illustrative key for the kinds of interaction among nanocomposite and protein receptors

CONCLUSIONS

1. Mushroom cultivation compost waste was employed as a natural source as a mediator for the creation of CuO@ZnO nanocomposite.
2. CuO@ZnO nanocomposite demonstrated notable anti-candidal activity, achieving inhibition zone 33.5 ± 2 mm and high anti-biofilm activity reaching 88.56%.
3. Based on the molecular docking data and efficiency of CuO-NPs and ZnO-NPs tested in this study, it can be concluded that the prepared NPs had therapeutic potential for targeting specific receptors and would be a more sensible pharmacological option for treating and inhibiting *C. albicans*.

ACKNOWLEDGMENTS

The authors extend their appreciation to Taif University, Saudi Arabia, for supporting this work through project number (TU-DSPP-2024-171).

Funding

This research was funded by Taif University, Saudi Arabia, project number (TU-DSPP-2024-171).

Conflicts of Interest

The authors state no conflict of interest.

REFERENCES CITED

Abdel-Ghany, T. M. (2013). "*Stachybotrys chartarum*: A novel biological agent for the extracellular synthesis of silver nanoparticles and their antimicrobial activity," *Indonesian J. Biotechnol*. 18(2), 75-82. DOI: 10.22146/ijbiotech.7871

Abdelghany, T. M., Al-Rajhi A. M., Mohamed, A. A., Alawlaqi, M. M., Magdah, M., Helmy, E. M., and Ahmed, S. M. (2018). "Recent advances in green synthesis of silver nanoparticles and their applications: About future directions. A review," *BioNanoScience* 8(1), 5-16. DOI: 10.1007/s12668-017-0413-3

Abdelghany, T. M., Bakri, M. M., Al-Rajhi, A. M. H., Al Abboud, M. A., Alawlaqi, M. M., and Shater, A. R. M. (2020). "Impact of copper and its nanoparticles on growth, ultrastructure, and laccase production of *Aspergillus niger* using corn cobs wastes," *BioResources* 15(2), 3289-3306. DOI: 10.15376/biores.15.2.3289-3306

Abdelghany, T. M., Al-Rajhi, A. M. H., Yahya, R., Marwah, M., Bakri, M. A., Al Abboud, Yahya, R., Husam, Q., Bazaid, A. S., and Salem, S. S. (2023a). "Phytofabrication of zinc oxide nanoparticles with advanced characterization and its antioxidant, anticancer, and antimicrobial activity against pathogenic microorganisms," *Biomass Conversion and Biorefinery* 13, 417-430. DOI: 10.1007/s13399-022-03412-1

Abdelghany, T. M., Al-Rajhi, A. M., Almuhayawi, M. S., Abada, E., Al Abboud, M. A., Moawad, H., Yahya, R., and Selim, S. (2023b). "Green fabrication of nanocomposite doped with selenium nanoparticle-based starch and glycogen with its therapeutic activity: Antimicrobial, antioxidant, and anti-inflammatory *in vitro*," *Biomass Conversion and Biorefinery* 13(1), 445-445. DOI: 10.1007/s13399-022-03257-8

Abdelhady, M. A., Abdelghany, T. M., Mohamed, S. H., and Abdelbary, S. A. (2024a). "Impact of green synthesized zinc oxide nanoparticles for treating dry rot in potato tubers," *BioResources* 19(2), 2106-2119. DOI: 10.15376/biores.19.2.2106-2119

Abdelhady, M., Abdelghany, T., Mohamed, S., and Abdelhamed, S. (2024b). "Biological application of zinc oxide nanoparticles created by green method," *Egyptian Journal of Soil Science* 64(3), 757-775. DOI: 10.21608/EJSS.2024.272650.1731

Al Abboud, M. A., Mashraqi, A., Qanash, H, Hattan S. G., Hashim R. F., Alkorbi, F., Mohamed, M. A., Tarek, M. A., and Moawad, H. (2024). "Green biosynthesis of bimetallic ZnO@AuNPs with its formulation into cellulose derivative: Biological and environmental applications," *Bioresour. Bioprocess* 11, 60. DOI: 10.1186/s40643-024-00759-3

Alghonaim, M. I., Alsalamah, S. A., Ali, Y., and Abdelghany, T. M. (2024a). "Green mediator for selenium nanoparticles synthesis with antimicrobial activity and plant biostimulant properties under heavy metal stress," *BioResources* 19(1), 898-916. DOI: 10.15376/biores.19.1.898-916

Alghonaim, M. I., Alsalamah, S. A., Mohammad, A. M., and Abdelghany, T. M. (2024b). "Green synthesis of bimetallic Se@TiO_2NPs and their formulation into biopolymers and their utilization as antimicrobial, anti-diabetic, antioxidant, and healing agent *in vitro*," *Biomass Conversion and Biorefinery* (Available Online). DOI: 10.1007/s13399-024-05451-2

Alghonaim, M. I., Alsalamah, S. A., Bazaid, A. S., and Abdelghany, T. M. (2024c). "Biosynthesis of CuO@Au NPs and its formulated into biopolymers carboxymethyl cellulose and chitosan: Characterizations, antimicrobial, anticancer and antioxidant Properties," *Waste and Biomass Valorization* (Available Online). DOI: 10.1007/s12649-024-02469-5

Alghonaim, M. I., Alsalamah, S. A., Alsolami, A., and Abdelghany, T. M. (2023). "Characterization and efficiency of *Ganoderma lucidum* biomass as an antimicrobial and anticancer agent," *BioResources* 18(4), 8037-8061. DOI: 10.15376/biores.18.4.8037-8061

Al-Rajhi, A. M. H., Yahya, R., Alawlaqi, M. M., Fareid, M. A., Amin, B. H., and Abdelghany, T. M. (2022a). "Copper oxide nanoparticles as fungistat to inhibit mycotoxins and hydrolytic enzyme production by *Fusarium incarnatum* isolated from garlic biomass," *BioResources* 17(2), 3042-3056. DOI: 10.15376/biores.17.2.3042-3056

Al-Rajhi, A. M. H., Yahya, R., and Bakri, M. M. (2022b). "*In situ* green synthesis of Cu-doped ZnO based polymers nanocomposite with studying antimicrobial, antioxidant and anti-inflammatory activities," *Applied Biological Chemistry* 65, article 35. DOI: 10.1186/s13765-022-00702-0

Al-Rajhi, A. M. H., and Abdelghany, T. M. (2023a). "*In vitro* repress of breast cancer by bio-product of edible *Pleurotus ostreatus* loaded with chitosan nanoparticles," *Applied Biological Chemistry* 66, article 33. DOI: 10.1186/s13765-023-00788-0

Al-Rajhi, A. M. H., and Abdelghany, T. M. (2023b). "Nanoemulsions of some edible oils and their antimicrobial, antioxidant, and anti-hemolytic activities," *BioResources* 18(1), 1465-1481. DOI: 10.15376/biores.18.1.1465-1481

Al-Rajhi, A. M. H., Alawlaqi, M. M., Abdel Ghany, T. M., and Moawad, H. (2023c). "*Amanita* sp. from subtropical region of Saudi Arabia as a source of chitinase enzyme and its antifungal activity," *BioResources* 18(2), 2928–2939. DOI: 10.15376/biores.18.2.2928-2939

Alsalamah, S. A., Alghonaim, M. I., Mohammad, A. M., and Abdel Ghany, T. M. (2023a). "Algal biomass extract as mediator for copper oxide nanoparticle synthesis: Applications in control of fungal, bacterial growth, and photocatalytic degradations of dyes," *BioResources* 18(4), 7474-7489. DOI: 10.15376/biores.18.4.7474-7489

Alsalamah, S. A., Alghonaim, M. I., Jusstaniah, M., and Abdelghany, T. M. (2023b). "Anti-yeasts, antioxidant and healing properties of Henna pre-treated by moist heat and molecular docking of its major constituents, chlorogenic and ellagic acids, with *Candida albicans* and *Geotrichum candidum* proteins," *Life* 13(9), article ID 1839. DOI: 10.3390/life13091839

Alsolami, A., Bazaid, A. S., Alshammari, M. A., Qanash, H., Amin, B. H., Bakri, M. M., and Abdelghany, T. M. (2023). "Ecofriendly fabrication of natural jojoba nanoemulsion and chitosan/jojoba nanoemulsion with studying the antimicrobial, anti-biofilm, and anti-diabetic activities *in vitro*," *Biomass Conversion and Biorefinery* (Available Online). DOI: 10.1007/s13399-023-05162-0

Antunes, F., Marçal, S., Taofiq O, Alcina, M. M. B., Morais, A. C., Isabel, C. F. R., and Manuela, P. (2020). "Valorization of mushroom by-products as a source of value-added compounds and potential applications," *Molecules* 25(11), article 2672. DOI: 10.3390/molecules25112672

BaQais, A., Alam, M. W., Farhan, M., Muteeb, G., Allag, N., and Mushtaq, S. (2023). "Probe-sonicated synthesis of CuO–ZnO hybrid nanocomposite for photocatalytic

and supercapacitor applications," *Inorganics* 11(9), article 370. DOI: 10.3390/inorganics11090370

Bekru, A. G., Tufa, L. T., Zelekew, O. A., Goddati, M., Lee, J., and Sabir, F. K. (2022). "Green synthesis of a CuO–ZnO nanocomposite for efficient photodegradation of methylene blue and reduction of 4-nitrophenol," *ACS Omega* 7(35), 30908-30919. DOI: 10.1021/acsomega.2c02687

El-Khawaga, A. M., Elsayed, M. A., Gobara, M., Suliman, A. A., Hashem, A. H., Zaher, A. A., Mohsen, M., and Salem, S. S. (2023). "Green synthesized ZnO nanoparticles by *Saccharomyces cerevisiae* and their antibacterial activity and photocatalytic degradation," *Biomass Conversion and Biorefinery* (Available Online). DOI: 10.1007/s13399-023-04827-0

El-Sayed, A. F., Aboulthana, W. M., Sherief, M. A., Gehan, T., El-Bassyouni G. T., and Mousa, S. M. (2024). "Synthesis, structural, molecular docking, and *in vitro* biological activities of Cu-doped ZnO nanomaterials," *Scientific Reports* 14, article 9027. DOI: 10.1038/s41598-024-59088-2

Elsakhawy T, Omara, A. E-D., Abowaly, M., El-Ramady, H., Badgar, K., Llanaj, X., Törős, G., Hajdú, P., and Prokisch J. (2022). "Green synthesis of nanoparticles by mushrooms: A crucial dimension for sustainable soil management," *Sustainability* 14(7), article 4328. DOI: 10.3390/su14074328

Frisch, M. J. E. A. (2009). Gaussian 09, Revision d. 01, Gaussian. Inc, Wallingford CT, 201.

Gur, T., Meydan, I., Seckin, H.; Bekmezci, M., and Sen, F. (2022). "Green synthesis, characterization and bioactivity of biogenic zinc oxide nanoparticles," *Environ. Res.* 204, article 111897. DOI: 10.1016/j.envres.2021.111897

Hemaid, A. S. S., Abdelghany, M. M. E., and Abdelghany, T. M. (2021). "Isolation and identification of *Candida* spp. from immunocompromised patients," *Bulletin of the National Research Centre* 45, article 163. DOI: 10.1186/s42269-021-00620-z

Kalantar E., Kabir, K., Gharibi, F., Hatami, S., and Maleki, A. (2013). "Effect and properties of surface-modified copper doped ZnO nanoparticles (Cu*:* ZnO NPs) on killing curves of bacterial pathogens," *Journal of Medical Bacteriology* 2(1-2), 20-26.

Khalid, A., Ahmad, P., Alharthi, A. I., Muhammad, S., Khandaker, M. U., Rehman, M., and Bradley, D. A. (2021). "Structural, optical and antibacterial efficacy of pure and zinc-doped copper oxide against pathogenic bacteria," *Nanomaterials* 11(2), article 451. DOI: 10.3390/nano11020451

Khalid, A., Ahmad, P., Alharthi, A. I., Muhammad, S., Khandaker, M. U., Faruque, M. R. I., Israf U. D., Mshari A. A., and Khan, A. (2021). "Synergistic effects of Cu-doped ZnO nanoantibiotic against Gram-positive bacterial strains," *Plos One* 16(5), article ID e0251082. DOI: 10.1371%2Fjournal.pone.0251082

Khan, S. A., Noreen, F., Kanwal, S., and Hussain, G. (2017). "Comparative synthesis, characterization of Cu-doped ZnO nanoparticles and their antioxidant, antibacterial, antifungal, and photocatalytic dye degradation activities," *Digest Journal of Nanomaterials and Biostructures and Biostructures* 12(3), 877-889.

Khoshkholgh-Pahlaviani, M. R. M., Massiha, A. R., Issazadeh, K., Bidarigh, S., Giahi, M., and Ramtin, M. (2013). "Evaluation of antifungal activity of methanol extract of Acacia (*Anagallis arvensis*) leaves and nystatin against *Candida albicans in vitro*," *Zahedan Journal of Research in Medical Sciences* 15(8), 39-41.

Lam, S. M., Quek, A. J., and Sin, J. C. (2018). "Mechanistic investigation of visible light responsive Ag/ZnO micro/nanoflowers for enhanced photocatalytic performance and

antibacterial activity," *Journal of Photochemistry and Photobiology A: Chemistry* 353, 171-184. DOI: 10.1016/j.jphotochem.2017.11.021

Mandal, S., Hazra, C., Joshi, N., Jain, N., Kumar, P., Sen, R., Das, S. and Das, K. (2024). "A comparison of chemical and biogenic surfactant mediated synthesis of ZnO/CuO: Highlighting the antimicrobial activity of the bio-functionalized metal oxide nanoparticles," *Colloids and Surfaces A: Physicochemical and Engineering Aspects* 690(5), article ID 133780. DOI: 10.1016/j.colsurfa.2024.133780

Mohamed, A. A., Abu-Elghait, M., Ahmed, N. E., and Salem, S.S. (2021). "Eco-friendly mycogenic synthesis of ZnO and CuO nanoparticles for in vitro antibacterial, antibiofilm, and antifungal applications," *Biological Trace Element Research* 199(7), 2788-2799. DOI: 10.1007/s12011-020-02369-4

Mohammadi-Aloucheh, R., Habibi-Yangjeh, A., Bayrami, A., Latifi-Navid, S., and Asadi, A. (2018). "Enhanced anti-bacterial activities of ZnO nanoparticles and ZnO/CuO nanocomposites synthesized using *Vaccinium arctostaphylos* L. fruit extract," *Artificial Cells, Nanomedicine, and Biotechnology* 46(Sup1), 1200-1209. DOI: 10.1080/21691401.2018.1448988

Mureed, S., Naz, S., Haider, A., Raza, A., Ul-Hamid, A., Haider, J., Ikram, M., Ghaffar, R., Irshad, M., Ghaffar, A., *et al.* (2021). "Development of multi-concentration Cu:Ag bimetallic nanoparticles as a promising bactericidal for antibiotic-resistant bacteria as evaluated with molecular docking study," *Nanoscale Research* 2021(1), article 91. DOI: 10.1186/s11671-021-03547-6

Papoutsis, K., Grasso, S., Menon, A., Brunton, N. P., Lyng, J. G., Jacquier, J.-C., and Bhuyan, D. J. (2020). "Recovery of ergosterol and vitamin D2 from mushroom waste - Potential valorization by food and pharmaceutical industries," *Trends in Food Science & Technology* 99, 351-366. DOI: 10.1016/j.tifs.2020.03.005

Qanash, H., Bazaid, A. S., Alharazi, T., Barnawi, H., Alotaibi, K., Shater, A. R. M., and Abdelghany, T. M. (2023). "Bioenvironmental applications of myco-created bioactive zinc oxide nanoparticle-doped selenium oxide nanoparticles," *Biomass Conversion and Biorefinery* 2023, 1-12. DOI: 10.1007/s13399-023-03809-6

Rafeeq, C. M., Paul, E., Vidya Saagar, E., and Manzur Ali, P. P. (2021). "Mycosynthesis of zinc oxide nanoparticles using *Pleurotus floridanus* and optimization of process parameters," *Ceram. Int.* 47, 12375-12380. DOI: 10.1016/j.ceramint.2021.01.091

Saied, M., Hasanin, M., Abdelghany, T. M., Amin, B. H., and Hashem, A. H. (2023). "Anticandidal activity of nanocomposite based on nanochitosan, nanostarch and mycosynthesized copper oxide nanoparticles against multidrug-resistant Candida," *International Journal of Biological and Macromolecules* 242, Article ID 124709. DOI: 10.1016/j.ijbiomac.2023.124709

Salama, A. M., Helmy, E. A., Abd El-ghany, T. M., and Ganash, M. (2021). "Nickel oxide nanoparticles application for enhancing biogas production using certain wastewater bacteria and aquatic macrophytes biomass," *Waste and Biomass Valorization* 12, 2059-2070. DOI: 10.1007/s12649-020-01144-9

Sandhya, J., and Kalaiselvam, S. (2021). "UV responsive quercetin derived and functionalized CuO/ZnO nanocomposite in ameliorating photocatalytic degradation of rhodamine B dye and enhanced biocidal activity against selected pathogenic strains," *Journal of Environmental Science and Health, Part A* 56(8), 835–848. DOI: 10.1080/10934529.2021.1930770

Shaheen, T. I., Fouda, A., and Salem, S. S. (2021). "Integration of cotton fabrics with biosynthesized CuO nanoparticles for bactericidal activity in the terms of their

cytotoxicity assessment," *Industrial and Engineering Chemistry Research* 60(4), 1553-1563. DOI: 10.1021/acs.iecr.0c04880

Ullah, H., Mushtaq, L., Ullah, Z., Fazal, A., and Khan, A. M. (2021). "Effect of vegetable waste extract on microstructure, morphology, and photocatalytic efficiency of ZnO−CuO nanocomposites," *Inorganic and Nano-Metal Chemistry* 51(7), 963-975. DOI: 10.1080/24701556.2020.1813766

Uyen, V. N., Anh, N. P., Van, N. T., Tri, N., Minh, N. V., Huy, N. N., Tran, V. L., Pag-Asa G., and Ha, H. K. (2020). "Characteristics and antifungal activity of CuO-ZnO nanocomposites synthesised by the sol-gel technique," *Vietnam Journal of Science, Technology and Engineering* 62(1), 17-22. DOI: 10.31276/VJSTE

Wahab, R., Khan, S. T., Dwivedi, S., Ahamed, M., Musarrat, J., and Al-Khedhairy, A. A. (2013). "Effective inhibition of bacterial respiration and growth by CuO microspheres composed of thin nanosheets," *Colloids and Surfaces B: Biointerfaces* 111, 211-217. DOI: 10.1016/j.colsurfb.2013.06.003

Yahya, R., Al-Rajhi, A. M., Alzaid, S. Z., Al Abboud, M. A., Almuhayawi, M. S., Al Jaouni, S. K., Selim, S., Ismail, K. S., and Abdelghany, T. M. (2022). "Molecular docking and efficacy of *Aloe vera* gel based on chitosan nanoparticles against *Helicobacter pylori* and its antioxidant and anti-inflammatory activities," *Polymers* 14, article 2994. DOI: 10.3390/polym14152994

Yousefinia, A., Khodadadi, M., and Mortazavi-Derazkola, S. (2023). "An efficient biosynthesis of novel ZnO/CuO nanocomposites using berberis vulgaris extract (ZnO/CuO@ BVENCs) for enhanced photocatalytic degradation of pollution, antibacterial and antifungal activity," *Environmental Technology and Innovation* 32, article ID 103340. DOI: 10.1016/j.eti.2023.103340

Zhu, L., Li, H., Liu, Z., Xia, P., Xie, Y., and Xiong, D. (2018). "Synthesis of the 0D/3D CuO/ZnO heterojunction with enhanced photocatalytic activity," *The Journal of Physical Chemistry C* 122(17), 9531-9539. DOI: 10.1021/acs.jpcc.8b01933

Article submitted: May 16, 2024; Peer review completed: July 1, 2024; Revised version received and accepted: July 7, 2024; Published: July 28, 2024.
DOI: 10.15376/biores.19.3.6670-6689